Synthesis, Crystal Structure and Magnetic Properties of Bixbyite-type Vanadium Oxide Nitrides

Suliman Nakhal[a], Wilfried Hermes[b], Thorsten Ressler[a], Rainer Pöttgen[b], and Martin Lerch[a]

[a] Institut für Chemie, TU Berlin, Straße des 17. Juni 135, 10623 Berlin, Germany
[b] Institut für Anorganische und Analytische Chemie and NRW Graduate School of Chemistry, Westfälische Wilhelms-Universität Münster, Corrensstraße 30, 48149 Münster, Germany

Reprint requests to M. Lerch. E-mail: lerch@chem.tu-berlin.de

Z. Naturforsch. **2009**, *64b,* 281 – 286; received December 12, 2008

Ammonolysis of vanadium sulfide leads to the formation of bixbyite-type vanadium oxide nitrides. Small amounts of nitrogen incorporated in the structure result in the stabilization of the bixbyite type not known for vanadium oxides. The crystal structure was investigated using X-ray diffraction and X-ray absorption spectroscopy. At temperatures above 550 °C the powders decompose to corundum-type V_2O_3 containing no detectable amount of nitrogen. Below 39 K magnetic ordering is observed.

Key words: Oxide Nitrides, Crystal Chemistry, Bixbyite

Introduction

In the last years nitrides and oxide nitrides have become shifted more and more in the focus of interest. In particular transition metal oxide nitrides are an interesting group of materials with physical properties making them candidates for technical applications. For example, they are candidates as photocatalysts for water splitting under sunlight [1 – 3]. Ionic conductivity studies focusing on the behavior of N^{3-} anions have yielded promising results indicating the possibility of N^{3-} ion conducting materials [4 – 6]. Transition metal oxide nitrides are also compounds possibly suitable as dielectrics [7, 8] in microelectronic devices, or as chemical gas sensors [9].

In contrast to the chemistry of oxide nitrides of transition metals such as tantalum or zirconium, where a lot of work was done in the last years, the knowledge of the related type of compounds of vanadium is not so extensive. More than thirty years ago Brauer and Reuther reported the first vanadium oxide nitrides [10], all structurally derived from the rock salt type. These non-stoichiometric compounds are metallic, and there is no evidence for magnetic ordering [11]. The possibility of a high-pressure synthesis of stoichiometric VON (a semiconductor) has been predicted by Lumey and Dronskowski [12].

In this contribution we report on the synthesis, crystal structure, and magnetic properties of vanadium oxide nitrides which can be formally described by partial substitution of oxygen by nitrogen in well-known vanadium sesquioxide. V_2O_3 displays a number of electronic, magnetic and structural properties that are challenging to interpret and explain [13 – 18]. At r. t. V_2O_3 exhibits the corundum structure, it is metallic and paramagnetic. It is unique among other isostructural sesquioxides with respect to its small a/c ratio and metallic conductivity. On reducing the temperature, corundum-type V_2O_3 shows a structural phase transition to a monoclinic structure at around 150 K. Accompanying the transition, a change from metallic to insulating behavior and the onset of antiferromagnetic ordering are observed. The metal-insulator transition is viewed as a Mott transition.

Experimental Section

Synthesis and chemical analysis

$V_{5.45}S_8$ is the basis compound the materials described in this study are derived from. It can be prepared by reacting V_2O_5 or NH_4VO_3 with flowing H_2S gas at 800 – 950 °C for 2 h. The vanadium sulfide obtained was converted into oxide nitrides by reaction with wet ammonia gas (3.8, Messer-Griesheim) at a constant flow rate of 15 – 20 L h^{-1} at temperatures of 325 – 500 °C for 20 h. EDX-analyses of the oxide nitrides obtained gave no indications for residual sulfur. Nitrogen and oxygen contents were determined using a LECO TC-300 / EF-300 N/O analyzer (hot gas extraction). The accuracy is ~ 2 % of the N/O contents present.

Structure determination

A Siemens D5000 powder diffractometer (Cu$K_{\alpha 1}$ radiation, $\lambda = 154.06$ pm, position-sensitive detector) was used for

0932–0776 / 09 / 0300–0281 $ 06.00

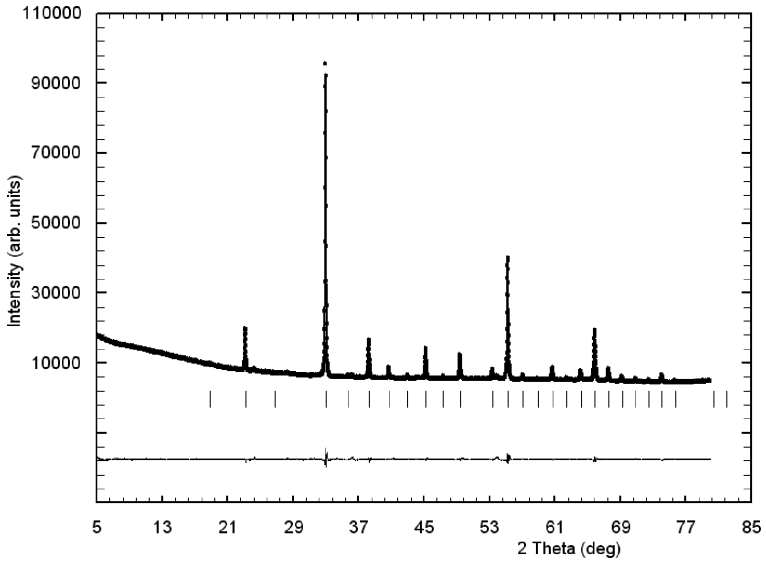

Fig. 1. X-Ray powder diffraction diagram of $V_2O_{3.07}N_{0.13}$ with the results of the Rietveld refinement.

the XRD measurements at r. t. Temperature dependent measurements (samples in SiO_2-glass capillaries under argon) were carried out using a Stoe STADI-P powder diffractometer (Mo$K_{\alpha 1}$ radiation, λ = 70.93 pm, imaging plate detector) with a graphite-heated resistance furnace. The program packages POWDER CELL 2.4 [19] and FULLPROF 2006 [20] were used for structural refinements. The peak profiles were fitted with a pseudo-Voigt function.

X-Ray absorption spectroscopy

In situ transmission XAS experiments were performed at the V K edge (5.465 keV, Si 111) at beamline E4 at the Hamburg Synchrotron Radiation Laboratory, HASYLAB. The storage ring operated at 4.4 GeV with injection currents of 150 mA. The materials were mixed with polyethylene ($\sim$ 5 mg oxide nitride (or oxide) and $\sim$ 30 mg PE) and pressed with a force of 2 t into a pellet (13 mm diameter). X-Ray absorption fine structure (XAFS) analysis was performed using the software WINXAS v3.1 [21]. Background subtraction and normalization were carried out by fitting linear polynomials to the pre-edge and the post-edge region of the absorption spectra, respectively. The extended X-ray absorption fine structure (EXAFS) data $\chi(k)$ was extracted by using cubic splines to obtain a smooth atomic background, $\mu_0(k)$. The pseudo radial distribution function FT($\chi(k) \times k^3$) was calculated by Fourier transforming the k^3-weighted experimental $\chi(k)$ function, multiplied by a Bessel window, into the R space. EXAFS data analysis was performed using theoretical backscattering phases and amplitudes calculated with the *ab initio* multiple-scattering code FEFF7 [22]. Single-scattering and multiple-scattering paths in the V_2O_3 model structure were calculated up to 6.0 Å with a lower limit of 2.0 % in amplitude with respect to the strongest backscattering path. EXAFS refinements were performed in R space simultaneously to the magnitude and the imaginary part of a Fourier transformed k^3-weighted and k^1-weighted experimental $\chi(k)$ data set using the standard EXAFS formula [23]. Structural parameters that have been determined by a least-squares refinement of a theoretical XAFS spectrum calculated for a V_2O_3 model structure to the experimental XAFS spectrum are (i) one overall E_0 shift, (ii) Debye-Waller factors for single-scattering paths, and (iii) distances of single-scattering paths. Coordination numbers (CN) and ${S_0}^2$ were kept invariant in the refinement.

Magnetic susceptibility measurements

The $V_2O_{3.07}N_{0.13}$ sample was packed in kapton foil and attached to the sample holder rod of a VSM for measuring the magnetic properties in a Quantum Design Physical-Property-Measurement-System in the temperature range 3 – 300 K with magnetic flux densities up to 80 kOe.

Results and Discussion

Bixbyite-type vanadium oxide nitrides in the composition range between $V_2O_{3.08}N_{0.02}$ and $V_2O_{3.07}$-$N_{0.13}$ have been prepared. As an example, an X-ray powder diffraction diagram of $V_2O_{3.07}N_{0.13}$ with the results of the Rietveld refinement is depicted in Fig. 1. Tables 1 and 2 present the refined structural data. In the well-known bixbyite-type structure, which can be considered a superstructure of the fluorite type, vanadium cations occupy the 8*a* (0, 0, 0) and 24*d*

Table 1. Refined structural data for $V_2O_{3.07}N_{0.13}$.

Structure type	bixbyite
Space group	$Ia\bar{3}$
Crystal system	cubic
Lattice parameter a, pm	939.66(1)
Unit cell volume V, pm^3	$829.69(2) \times 10^6$
Formula units Z	16
Calculated density ρ, g cm^{-3}	4.89
Diffractometer	Siemens D5000
Wavelength, pm	154.06
2θ range, deg	5 – 80
R_{wp}	0.022
R_{Bragg}	0.009
R_{exp}	0.012
S	1.67

Table 2. Refined atomic parameters for $V_2O_{3.07}N_{0.13}$.

Atom	W. site	x	y	z	B_{iso} (Å^2)
V1	8*a*	0	0	0	1.5(1)
V2	24*d*	0.2823(1)	0	1/4	1.42(7)
O/N	48*e*	0.1422(4)	0.1290(5)	−0.0944(3)	0.86(7)

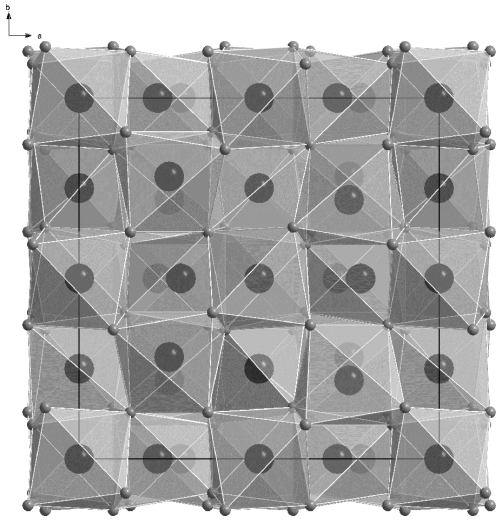

Fig. 2. Unit cell of bixbyite-type $V_2O_{3.07}N_{0.13}$ with the connectivity of the $V(O/N)_6$ octahedra.

$(x, 0, 1/4)$ Wyckoff positions, and the oxide/nitride anions the general position 48*e*. Fig. 2 shows the unit cell. All cations are octahedrally coordinated by six anions, which are surrounded tetrahedrally by four vanadium ions. Details are given in Fig. 3 and Table 3. The bixbyite type is also known from other transition metal oxide nitrides, for example Zr_2ON_2 and Hf_2ON_2 [24 – 27], and from $V_2O_{2.70}N_{0.15}F_{0.15}$ [28]. From the oxide nitride compounds it is also known that the bixbyite structure tolerates a partial occupation of the anion vacancies, which are fully occupied

Table 3. Type and number (N) of atoms at distance R from the V center in $V_2O_{3.07}N_{0.13}$ obtained from a refinement of a bixbyite model structure (Tables 1 and 2) to the experimental V K edge XAFS functions $\chi(k)$ (k ranges from 2.0 to 11.1 Å^{-1}, R ranges from 1.1 to 5.1 Å, $S_o{}^2 = 0.9$ (fix), $E_0 = -6.0$ eV, residual = 4.9, $N_{ind} = 25$, $N_{free} = 20$). The uncertainty in the distances amounts to about 0.03 Å.

Type	N	R (Å) model V_2O_3	R (Å) $V_2O_{3.07}N_{0.13}$	σ^2 (Å^2) $V_2O_{3.07}N_{0.13}$
V–O	2	1.97	1.902	0.0254
V–O	2	2.01	1.998	0.00318
V–O	2	2.06	2.026	0.00127
V–V	2	3.12	3.116	0.00392
V–V	4	3.13	3.123	0.00734
V–V	4	3.54	3.55	0.00692
V–V	2	4.70	4.698	0.00271

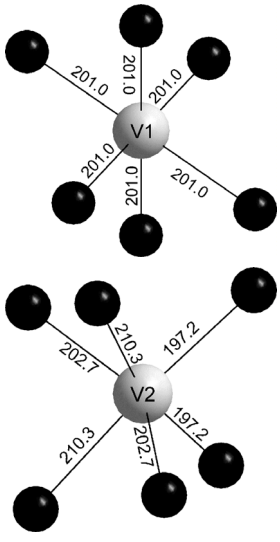

Fig. 3. $V(O/N)_6$ octahedra in $V_2O_{3.07}N_{0.13}$ with the bond lengths (pm) determined.

in the ideal fluorite structure (AX_2 type), leading to deviations from the ideal bixbyite composition A_2X_3. Unfortunately, it has not been possible to refine the occupation of the 16*c* (1/8, 1/8, 1/8) position (empty in ideal A_2X_3 bixbyite structures) by 'additional' anions using X-ray powder methods.

The V K edge XANES spectra of V_2O_3 (corundum) and $V_2O_{3.07}N_{0.13}$ are depicted in Fig. 4. Compared to the XANES spectrum of corundum-type V_2O_3, the XANES spectrum of $V_2O_{3.07}N_{0.13}$ exhibits a slightly higher characteristic pre-edge peak. The latter can be employed to estimate the average oxidation state of vanadium in $V_2O_{3.07}N_{0.13}$. In comparison to the reference compounds V_2O_3 and V_2O_5 the average valence of V in $V_2O_{3.07}N_{0.13}$ amounts to 3.25. Both the average "valence" and the distortion of the local coordination influence the pre-edge peak height. Hence, the

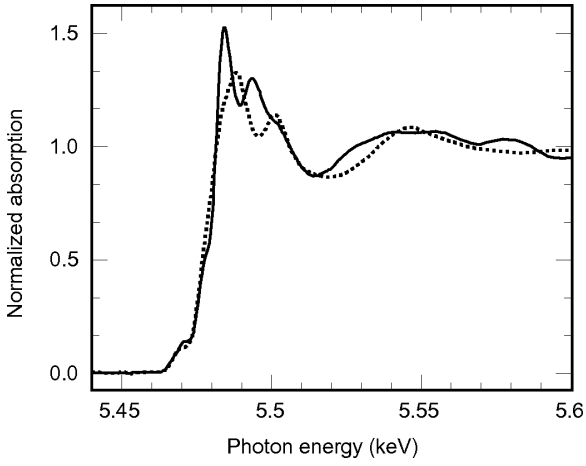

Fig. 4. Comparison of the V *K* edge XANES spectra of corundum-type V_2O_3 (dotted line) and bixbyite-type $V_2O_{3.07}N_{0.13}$ (solid line).

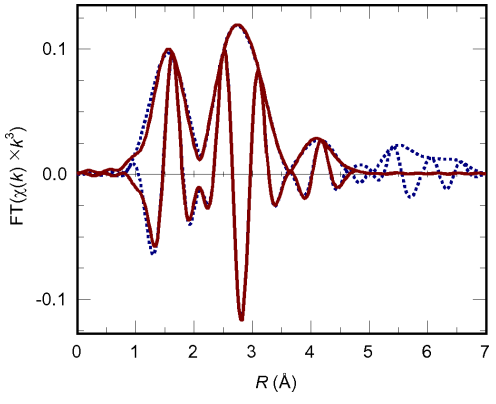

Fig. 5. Refinement of the theoretical XAFS function based on the bixbyite-type model structure (Tables 1 and 2) (solid line) to the experimental V *K* edge FT($\chi(k) \times k^3$) of $V_2O_{3.07}N_{0.13}$ (dotted line).

uncertainty in the average "valence" is estimated to be about 0.05. Provided that each nitrogen atom incorporated in the V_2O_3 structure results in an oxidation of one V^{3+} center to a V^{4+} center, the expected average formal oxidation state of vanadium in $V_2O_{3.07}N_{0.13}$ amounts to +3.26.

The Fourier-transformed XAFS $\chi(k) \times k^3$ of $V_2O_{3.07}N_{0.13}$ is depicted in Fig. 5. The pronounced amplitude of the V–V shells at higher distances (> 2 Å) confirms the crystallinity and the well-defined structure of $V_2O_{3.07}N_{0.13}$. The experimental FT($\chi(k) \times k^3$) of $V_2O_{3.07}N_{0.13}$ can be very well simulated using a calculated FT($\chi(k) \times k^3$) based on the bixbyite model structure given in Tables 1 and 2. The good agreement

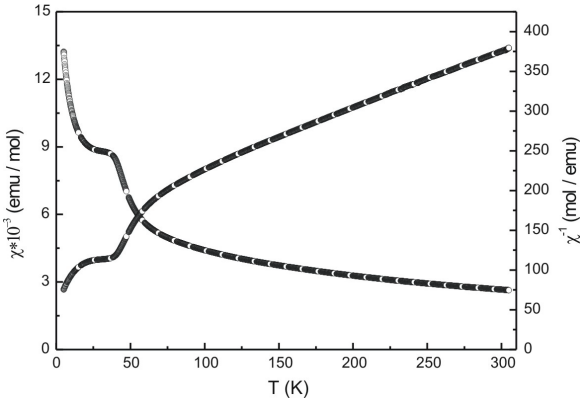

Fig. 6. Temperature dependence of the magnetic and inverse magnetic susceptibility of $V_2O_{3.07}N_{0.13}$ measured at a flux density of 40 kOe.

of the experimental and theoretical spectrum in Fig. 5 excludes the presence of considerable amounts of additional crystalline or amorphous phases in the material studied. The local structural parameters as determined from the XAFS refinement are given in Table 3. The minor deviations between the model and the refined parameters confirm the good agreement between the long-range and short-range ordered structure of $V_2O_{3.07}N_{0.13}$.

The temperature dependence of the magnetic and inverse magnetic susceptibility of the $V_2O_{3.07}N_{0.13}$ sample is presented in Fig. 6. The susceptibilities were found to be slightly field-dependent. The 30 and 40 kOe data were already identical in the paramagnetic range. $V_2O_{3.07}N_{0.13}$ shows Curie-Weiss behavior in the temperature range 100 to 300 K, resulting in an experimental magnetic moment of μ_{eff} = 2.36(3) μ_B per V atom and a Weiss constant of $\theta_P = -214(5)$ K. The experimental magnetic moment is in between the values of μ_{theo} (V^{3+}) = 2.83 μ_B and μ_{theo} (V^{4+}) = 1.73 μ_B. The susceptibility data nicely confirm the XANES measurements which revealed an oxidation state of +3.26.

Below *ca.* 39 K we have observed magnetic ordering. The magnetization shows complex temperature- and field-dependent behavior. These phenomena are not yet understood and will be reported and discussed in a forthcoming manuscript. Compared with pure V_2O_3 (antiferromagnetic ordering in the range 150–162 K through a metal-insulator transition [14, 29–31]) we have observed a drastic drop in the ordering temperature for $V_2O_{3.07}N_{0.13}$. More detailed studies on the magnetic behavior are in progress.

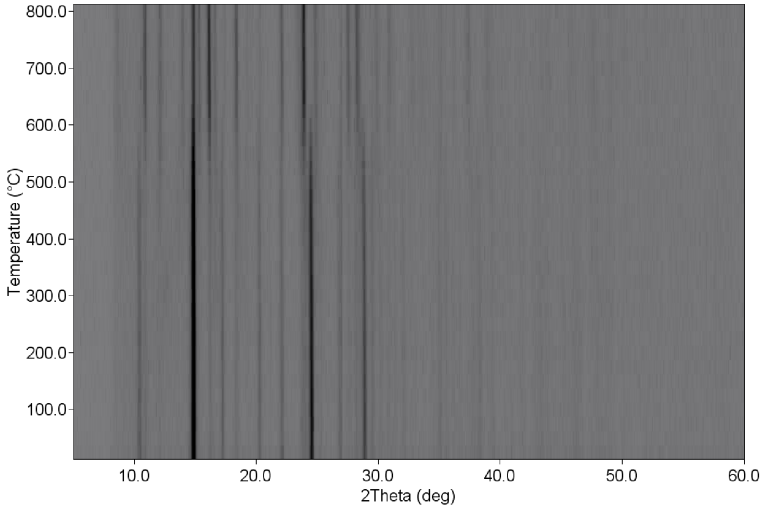

Fig. 7. High-temperature X-ray powder patterns of bixbyite-type $V_2O_{3.07}N_{0.13}$ in argon atmosphere. Above $\sim$ 550 °C a corundum-type phase (V_2O_3) is observed.

At high temperatures bixbyite-type vanadium oxide nitrides decompose. In inert gas atmosphere at $\sim$ 550 °C a 'transformation' (better decomposition) to a corundum-type structure was observed by high-temperature XRD measurements (Fig. 7). The resulting phase contains no nitrogen. In air, an oxidation to V_2O_5 was observed at around 350 °C.

Conclusions

Vanadium oxide nitrides containing a small amount of nitrogen exhibit crystal structures not known for the pure oxides. This partial substitution can therefore be considered as a general route to new materials with interesting physical properties which has to be investigated in more detail. The bixbyite-type oxide nitride presented here is just one of several examples. In the near future we will report on a vanadium oxide nitride showing the pseudobrookite-type structure.

Acknowledgements

The authors thank B. Hahn for N/O analysis, M. Borowski for temperature-dependent X-ray measurements, and J. Nissen (ZELMI) for EDX analysis. W. H. is indebted to the Fonds der Chemischen Industrie for a PhD stipend. HASYLAB, Hamburg, is acknowledged for providing beamtime.

[1] S. Ito, K. R. Thampi, P. Comte, P. Liska, M. Grätzel, *Chem. Commun*. **2005**, 268.
[2] M. Hara, T. Takata, J. N. Kondo, K. Domen, *Catal. Today* **2004**, *90*, 313.
[3] R. Nakamura, T. Tanaka, Y. Nakato, *J. Phys. Chem. B* **2005**, 8920.
[4] M. Lerch, J. Lerch, R. Hock, J. Wrba, *J. Solid State Chem*. **1997**, *128*, 282.
[5] J. Wendel, M. Lerch, W. Laqua, *J. Solid State Chem*. **1999**, *142*, 163.
[6] M. A. Taylor, M. Kilo, C. Argirusis, G. Borchardt, I. Valov, C. Korte, J. Janek, T. C. Roedel, M. Lerch, *Solid State Data, Pt. A: Defect and Diffusion Forum* **2005**, *237–240*, 479.
[7] J. H. Swisher, M. H. Read, *Metal. Trans*. **1972**, *3*, 489.
[8] M. Kerlau, O. Merdrignac-Conanec, M. Guilloux-Viry, A. Perrin, *Solid State Sci*. **2004**, *6*, 101.
[9] O. Merdrignac-Conanec, M. Kerlau, M. Guilloux-Viry, R. Marchand, N. Barsan, U. Weimar, *Silicates Indust*. **2004**, *69*, 141.
[10] G. Brauer, H. Reuther, *Z. Anorg. Allg. Chem*. **1973**, *395*, 151.
[11] B. Wang, B. C. Chakoumakos, B. C. Sales, J. B. Bates, *J. Solid State Chem*. **1996**, *122*, 376.
[12] M. W. Lumey, R. Dronskowski, *Z. Anorg. Allg. Chem*. **2005**, *631*, 887.
[13] D. B. McWhan, T. M. Rice, J. P. Remeika, *Phys. Rev. Lett*. **1969**, *23*, 1334.
[14] P. D. Dernier, M. Marezio, *Phys. Rev. B* **1970**, *2*, 3771.
[15] R. M. Moon, *Phys. Rev. Lett*. **1970**, *25*, 527.
[16] D. B. McWhan, A. Menth, J. P. Remeika, W. F. Brinkman, T. M. Rice, *Phys. Rev. B* **1973**, *7(5)*, 1920.
[17] T. M. Rice, *Spectroscopy of Mott Insulators and Correlated Metals*, (Eds.: A. Fujimori, Y. Tokura), Springer, Berlin, **1995**.
[18] F. Mila, R. Shiina, F.-C. Zhang, A. Joshi, M. Ma, V. Anisimov, T. M. Rice, *Phys. Rev. Lett*. **2000**, *85(8)*, 1714.
[19] W. Kraus, G. Nolze, Bundesanstalt für Materialprüfung (BAM), Berlin (Germany) **2000**.

[20] J. Rodríguez-Carvajal, FULLPROF 2006, A. Program for Rietveld Refinement and Pattern Matching Analysis, **2006**; see also: Satellite Meeting on Powder Diffraction of the 15th International Congress of the IUCr, Toulouse (France) **1990**, p. 127; J. Rodríguez-Carvajal, *Physica B* **1993**, *192*, 55.
[21] T. Ressler, *J. Synch. Rad*. **1998**, *5*, 118.
[22] J. J. Rehr, C. H. Booth, F. Bridges, S. I. Zabinsky, *Phys. Rev. B* **1994**, *49*, 12347.
[23] T. Ressler, S. L. Brock, J. Wong, S. L. Suib, *J. Phys. Chem. B* **1999**, *103*, 6407.
[24] J. C. Gilles, *Bull. Soc. Chim. Fr*. **1962**, 2118.
[25] E. Füglein, R. Hock, M. Lerch, *Z. Anorg. Allg. Chem*. **1997**, *623*, 304.
[26] S. J. Clarke, C. W. Michie, M. J. Rosseinsky, *J. Solid State Chem*. **1999**, *146*, 399.
[27] T. Bredow, M. Lerch, *Z. Anorg. Allg. Chem*. **2004**, *630*, 2262.
[28] B. Tanguy, M. Pezat, A. Wold, J. Portier, *C. R. Acad. Paris C* **1976**, *282*, 291.
[29] R. M. Moon, *Phys. Rev. Lett*. **1970**, *25*, 527.
[30] D. B. McWhan, A. Menth, J. P. Remeika, W. F. Brinkman, T. M. Rice, *Phys. Rev. B* **1973**, *7*, 1920.
[31] B. Sass, C. Tusche, W. Felsch, F. Bertran, F. Fortuna, P. Ohresser, G. Krill, *Phys. Rev. B* **2005**, *71*, 014415.